Journal of Renewable Materials

Tech Science Press

https://doi.org/10.32604/jrm.2026.02026-0221

ARTICLE

Effect of Modified Gum Arabic and Euphorbia Trigona Mill Master Batch on the Crystallization and Thermal Stability of Poly (Lactic Acid)

Kasahun Tsegaye Mekonnen[1,*], Melaku Tesfaye Alemea[2], Dessie Ezez[1], Abenezer Zenebe[1] and Negussie Darota Daka[1]

[1]Department of Chemistry, College of Natural and Computational Science, Arba Minch University, Arba Minch, Ethiopia
[2]Department of Chemical Engineering, Adama Science and Technology University, Adama, Ethiopia

*Corresponding Author: Kasahun Tsegaye Mekonnen. Email: kaschem2121@gmail.com

Received: 24 November 2025; Accepted: 09 April 2026; Published: 28 May 2026

ABSTRACT: This study examined the effects of modified Gum Arabic (OLLA-g-GA), modified *Euphorbia trigona* Mill (OLLA-g-ETML), and their master batch (OLLA-g-GA–OLLA-g-ETML) on the non-isothermal crystallisation and thermal stability of poly (lactic acid) (PLA). The interface interactions of PLA with the modifiers before and after modification were analysed and identified using FTIR spectroscopy, which displayed different peak formations and intensities compared to neat PLA, indicating physical interactions with the modifiers. Differential scanning calorimetry (DSC) was used to study non-isothermal crystallisation at a heating rate of 10°C/min. Tensile strength and elongation at break of PLA improved by the addition of biofiller. The incorporation of OLLA-g-GA, OLLA-g-ETML, and their master batch enhanced the crystallinity enhancement to 39.32%, 36.30%, and 40.39%, respectively, from 31.36% (for neat PLA) to 35.28%. Thermal annealing increased the crystallinity of the PLA/master batch composites to 45.83%. These findings confirm that blending PLA with modified gum Arabica, *Euphorbia trigona* Mill, and master batch had a positive effect on the crystallisation and thermal stability of PLA, demonstrating a successful methodology for improving the performance of biodegradable polymer composites.

KEYWORDS: Gum Arabic; euphoria trigona mill; master batch; thermal stability; poly (lactic acid)

1 Introduction

The global shift towards sustainable alternatives is in part due to the growing environmental impact of petroleum-based polymers [1,2]. The biodegradability of biopolymers and their lower environmental impact have made bio-based polymers valued as substitutes. Currently, polycaprolactone(PCL) [3], poly(lactic acid) (PLA) [4], and polyhydroxybutyrate (PHB) are being studied for packaging and biomedical uses [5]. Among these, polylactic acid (PLA) is notable for its considerable stiffness, good strength, ease of processing, and non-toxic combustion [6].

Despite having the advantage, PLA suffers from inherent deficiencies such as slow crystallisation kinetics, low crystallinity, and poor thermal stability, which limit its use in high temperature application and in applications requiring barrier properties [7]. These shortcomings can be mitigated by the incorporation of various polymers [8], plasticisers [9] and natural fillers [10], which improve their thermal, mechanical and crystallisation properties.

Biopolymer-derived natural fillers such as starch, cellulose, and gum arabic have been widely investigated for use in reinforcing PLA [11,12]. However, challenges like agglomeration of the filler and degradation

of the matrix due to excessive surface functionality typically ruin composite performance when melt processing. To overcome these obstacles, different strategies like surfactant treatment, addition of coupling agent, grafting agent and compatibiliser can be employed [13].

Grafting using moieties such as acrylic acid, caprolactone, oxazoline, glycidyl methacrylate, and lactic acid are some examples that have been employed in this respect [14]. The application of lactic acid as a grafting agent for polymer-containing polymer gum Arabica(GA) is widely used. By crosslinking, it enhances the mechanical, thermal, and interfacial adhesion of PLA and modified GA [15]. Additionally, it maintains biodegradability and facilitates GA dispersion in PLA composites.

Despite the fact that many studies have proved that chemically modified G A serves as an effective nucleating agent for enhancing the crystallisation behavior of PLA, there has been a concentration of most studies on a single filler system [16]. The combined effect of hydrophobically modified GA and ETML, especially via a masterbatch approach, has not yet been systematically studied. Moreover, there has been very little emphasis on how such hybrid systems of natural fillers influence the non-isothermal crystallization characteristics and thermal degradation kinetics of PLA. Consequently, further research is required to design PLA-based composites with improved thermal stability and predictably controlled crystallisation characteristics.

Therefore, the objective of this study is to evaluate the individual and combined contributions of chemically modified Gum Arabic (OLLA-g-GA), modified *Euphorbia trigona* Mill (OLLA-g-ETML), and their masterbatch system on the non-isothermal crystallisation behavior and thermal degradation kinetics of PLA. Through differential scanning calorimetry (DSC), the cold crystallisation behavior will be evaluated, while thermogravimetric analysis (TGA) will be conducted to examine thermal stability. The work aims to elucidate the synergistic effects of modified natural plant fillers.

2 Exprimental

2.1 Materials

For the present investigation, polylactic acid (PLA) pellets of the 4032D type used in this study were supplied by Nature Works LLC (USA) and had a specific gravity of 1.24 and a melt mass flow rate (MFR) of 7 g/10 min at 210°C/2.16 kg. They were used as the polymer matrix. Gum Arabica (GA) was purchased from Sisco Research Laboratories Pvt. Ltd. (Maharashtra, India), chloroform (99.99%, Fisher Chemicals Scientific UK), L-lactic acid (88% aqueous solution, analytical-reagent grade, Loba Chemie Pvt. Ltd. chemical manufacturer in Mumbai, India), analytical grade chloroform were used as a solvent and *Euphorbia trigona* latex (ETML) collected from mature *Euphorbia trigona* plants in Adama city, Ethiopia, filtered to remove debris, and used fresh. The sample designations and compositions of the prepared PLA-based systems are summarized in Table 1.

Table 1: Sample designation and composition.

Sample Code	PLA (wt%)	OLLA-g-GA (wt%)	OLLA-g-ETML (wt%)	Masterbatch
PLA	100	0	0	No
PLA/OLLA-g-GA	97	3	0	No
PLA/OLLA-g-ETML	95	0	5	No
PLA/masterbatch(OLLA-g-GA–OLLA-g-ETML)	92	3	5	Yes

2.2 Synthesis of OLLA-g-GA and OLLA-g-ETML Bio-Conjugate via Graft Polymerization

The grafting of OLLA into GA was performed under controlled polycondensation conditions. As outlined in [17], the procedure was as follows, a mixture of lactic acid and GA in a weight ratio of 1:10 was manually homogenised in a round-bottom flask as illustrated in Fig. 1. This mixture was then heated and maintained at 168°C for 2.5 h after which the reactor was allowed to cool to room temperature, and the bioconjugate was isolated. The crude bioconjugate was then purified from the unreacted lactic acid by extensive washing with water. The purified OLLA-g-GA conjugate formed a highly viscous liquid upon cooling and was stored in a sealed container for subsequent analysis.

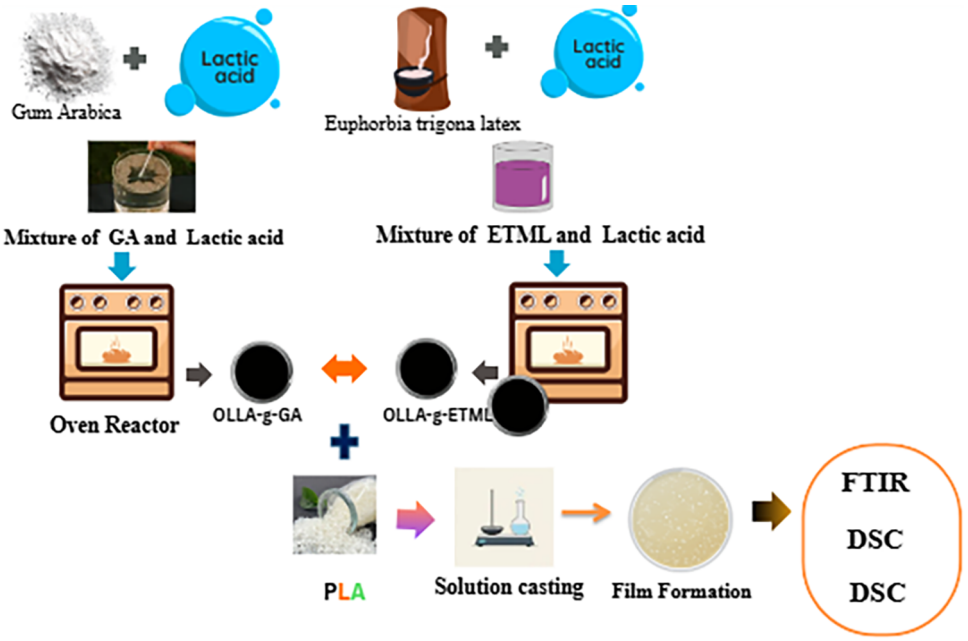

Figure 1: Preparation mechanism of bio-conjugate and PLA based biocomposite film.

On the contrary, OLLA-g-ETML has also been obtained through the polycondensation of lactic acid and ETML in round bottom flask with a 1:3 wt% ratio, as indicated by unpublished results of Yemisarch (2021). In this process, the mixture was heated to 150°C for a period of 3 h. For graft polymerisation, lactic acid was reacted with Gum Arabic at a weight ratio of 1:10 to form OLLA-g-GA, while lactic acid and Euphorbia tirgona mill latex were reacted at a 1:3 weight ratio to obtain OLLA-g-ETML. The bio-conjugate was collected following the cooling process and washed with distilled water to remove unreacted lactic acid, ultimately becoming a viscous liquid at room temperature. The purified OLLA-g-ETML conjugate formed a highly viscous liquid upon cooling and was stored in a sealed container for subsequent analysis. The synthesised OLLA-g-GA and OLLA-g-ETML bioconjugates were subsequently used as bio-based modifiers for PLA in the preparation of PLA blends and masterbatches.

2.3 Preparation of PLA Bio-Composite Films

Biopolymer films were prepared through the solution casting method. Modified gums (OLLA-g-GA), modified euphorbia trigon mill (OLLA-g-ETML) and master bath (OLLA-g-GA + OLLA-g-ETML mixed with PLA solution as shown in Fig. 1. Based on the PLA mass, PLA/OLLA-g-GA (3%), PLA/OLLA-g-ETML (5%) and PLA-OLLA-g-GA (3%)-OLLA-g-ETML (5%)) were prepared through the solution casting method. A 3% OLLA-g-GA, 5% OLLA-g-ETML and master batch were mixed separately with pre-dissolved PLA

(3 g) in chloroform (90 mL) with vigorous stirring magnetically at a rotational speed of 20 rps at room temperature. Each solution was poured into Petri dishes and films were peeled off from the Petri dishes after 48 h. In a similar way neat PLA films were also prepared.

2.4 Experimental Protocol for Characterisations of Bio-Conjugate

2.4.1 Grafting Calculation

The extent of grafting was quantitatively evaluated to determine the efficiency of oligomeric lactic acid (OLLA) attachment onto Gum Arabic (GA) and *Euphorbia trigona* Mill latex (ETML). The grafting percentage (GP) was calculated according to the following relation:

$$\text{Grafting Percentage (GP)} = \left(\frac{W1 - Wo}{Wo} \times 100\right) \quad (1)$$

$$\text{Grafting efficiency (GE)} = \left(\frac{W1 - Wo}{W2} \times 100\right) \quad (2)$$

where, W_0: weight of neat substrate (GA or ETML); W_1: weight of grafted copolymer after purification; W_2: weight of lactic acid (monomer) used in the reaction.

To ensure consistent results, all measurements were taken three times and averaged before being reported. The grafting parameters were quantifiable. This information could also be used to compare OLLA grafting on GA and ETML. A quantitative relationship existed between the two. Subsequent structural and functional characterisations of the bioconjugates would provide further insights into the grafting.

2.4.2 Nuclear Magnetic Resonance (NMR) Characterization of OLLA, OLLA-g-GA, ETMl and OLLA-g-ETML

Proton nuclear magnetic resonance (^{1}H NMR) analyses were carried out on the OLLA, *OLLA-g*-GA, ETML and OLLA-g-ETML samples by using Bruker Ascend^{TM} 600 nuclear magnetic resonance spectrometer to analyse lactic acid grafting GA and ETML. The OLLA, OLLA-g-GA of ~10 mg/mL concentration was prepared by dissolving the samples in deuterated chloroform ($CDCl_3$). The prepared solutions were filtered and transferred into NMR tubes for analysis at room temperature. Similarly done for ETML and OLLA-g-ETML. For ^{1}H NMR, chloroform (at 7.26 ppm) was used as the reference.

2.5 Experimental Protocol for Characterizations of Bio-Films

2.5.1 Fourier Transformed Infrared Spectroscopy (FTIR)

The Spectrum FTIR (Make: Frontier, Perkin Elmer) is used to gather FTIR spectra of materials. Attenuated Total Reflectance (ATR) assembly is used to record infrared spectra in transmission mode. A KBr crystal with a wavenumber between 4000 and 600 cm^{-1} is covered with extruded film. Before analysis, a background spectrum is gathered in order to remove spectra and offset the effects of airborne carbon dioxide and humidity. FTIR analysis is performed to look into any potential interactions between the PLA and the master batch, OLLA-g-GA (3%), and OLLA-g-ETML (5%) before and after thermal annealing.

2.5.2 Mechanical Characteristics

Before preparing the sample for the test, the bio composite films of PLA/*OLLA-g*-GA, PLA/*OLLA-g*-ETM and PLA/*OLLA-g*-GA-*OLLA-g*-ETM (master batch) were conditioned overnight, under a conditioning oven at 20°C and 65.78% humidity. After this step sample was prepared in a 100 cm length by 13 cm width by using a ruler, pen (marker) and scissors. This test was performed by the Ethiopian Conformity Assessment

Enterprise, following the ASTM D638 tensile strength measuring procedure using a universal tensile strength testing machine. The force at break and tensile strength was done simultaneously.

2.5.3 Differential Scanning Calorimeter (DSC)

Crystallization and melting behavior studies of neat PLA and PLA based bio composites were investigated on a differential scanning calorimeter (DSC). DSC measurements of the neat PLA, PLA-*OLLA*-*g*-GA (3%) *PLA*-*OLLA*-*g*-ETUM (5%) master batch PLA-*OLLA*-*g*-GA (3%)-*OLLA*-*g*-ETUM (5%) after annealing time of 30 min 1:30 h and 2.5 h were performed on DSC Q200 (TA Instruments, New Castle, DE, USA) over a temperature range from 25 to 200°C at a heating rate of 10°C/min and then held for 5 min, and then samples were cooled down to 25°C at a cooling rate of 5°C/min. To find the glass transition temperature (T_g), crystallization temperature (T_c), and melting temperature (T_m), a second heating was carried out at the same range and heating rate. The degree of crystallinity of neat PLA and PLA-based biocomposite was determined using Eqs. (3) and (4), respectively.

$$X_C = \frac{\Delta H_m}{\Delta H_m^\circ} * 100 \tag{3}$$

$$Xc = \left(\frac{\Delta \mathrm{Hm}}{Wf \times \Delta \mathrm{Hmo}} \right) \times 100 \tag{4}$$

where ΔHm is the melting enthalpy, ΔHm ^{o} is the 100% crystalline melting enthalpy for PLA and 100% crystalline PLA and *Wf* is the polymer weight fraction in the blend.

2.5.4 Thermal Annealing Protocol

In order to examine the influence of annealing time on crystallisation behavior of PLA-based biocomposites, a thermal annealing of all the composite samples was conducted under isothermal conditions. Annealing was performed at 110 C, having temperatures above the glass transition temperature and below the melting temperature of PLA, and the time of annealing was adjusted (30, 60, 90 and 150 min). The samples were then allowed to cool to ambient temperature after annealing under controlled conditions so as to maintain the formed crystalline structure.

2.5.5 Thermal Gravimetric Analysis of Bio-Composite

Thermal stability of the synthesized neat PLA, master batch PLA/*OLLA*-*g*-GA (3%)-*OLLA*-*g*-ETML (5%) and bio-composite (PLA-*OLLA*-*g*-GA (3%)-*OLLA*-*g*-ETML (5%)) were determined by thermo gravimetric analysis. The analysis was performed in the range from 25°C to 700°C at a rate of 10°C/min heating range under a controlled inert atmosphere by measuring their mass as a function of temperature. In order to prepare thin films for the optical microscope, the composite was melted on a glass slide at 150°C for 10 min and another glass slide was placed on top of the melted samples as a cover glass to create a flat thin film for each formulation. The behavior of weight mass loss and decomposition temperature was observed from the TGA thermograph using iSolution DT software.

3 Results and Discussion

3.1 Grafting Calculation

The grafting percentage (GP) and grafting efficiency (GE) of the synthesized bioconjugates are summarized in Table 2. Among the samples, GA-g-OLLA exhibited a GP of 21.5 ± 0.56% and a GE of 67.2 ± 0.89%, indicating effective OLLA grafting onto the gum arabic backbone. In comparison, ETML-g-OLLA

depicted a higher GP of 24.3 ± 0.33% and GE of 73.6 ± 0.47%, implying the ETML modification improves the grafting efficiencies. These values are consistent with previously reported polysaccharides–lactic acid grafting systems [18], confirming the successful synthesis of the bioconjugate.

Table 2: Grafting percentage and grafting efficiency of GA, ETML, OLLA, OLLA-g-GA, and OLLA-g-ETML.

Sample	GP	GE
GA-g-OLLA	21.5 ± 56	67.2 ± 89
ETML-g-OLLA	24.3 ± 33	73.6 ± 47

3.2 Structural Analysis of OLLA Bio Conjugates, Modified GA and Modified ETML

The ^{1}H-NMR Spectrum of OLLA shows methyl multiplets at δ 1.43–1.55 ppm (CH_3 lactyl units)(d) as illustrated in Fig. 2. Signals from the methine backbone appear at δ 4.28–4.38 ppm (CH bonded to either one of the esters or a CH_3)(c) and end-group sensitive methane signal at δ 5.10–5.16 ppm (OH-terminated or esterified COOH ends)(b), confirming that they have an oligolactic structure. A minor additional signal (at δ 6.77 ppm)(d), but it is not attributable to the lactic backbone therefore it is either a non-diagnostic impurity or an exchange feature. The total transversal diffusion of peaks without a carboxylic acid proton (δ 11–12 ppm) suggests that the lactic acid monomer did not interact with other subunits. Therefore, the lactic acid monomer did not interact with other subunits. These characteristics affirm the polycondensation to oleomeric OLLA lactic acid [19].

(a) Peak at δ = 6.77 ppm, corresponding to aromatic protons in the OLLA moiety.
(b) Multiplet at δ = 5.10–5.16 ppm, assigned to methine protons adjacent to ester linkages.
(c) Multiplet at δ = 4.20–4.38 ppm, representing methylene protons near oxygen atoms.
(d) Multiplet at δ = 1.43–1.55 ppm, attributed to aliphatic methylene protons in the OLLA backbone.

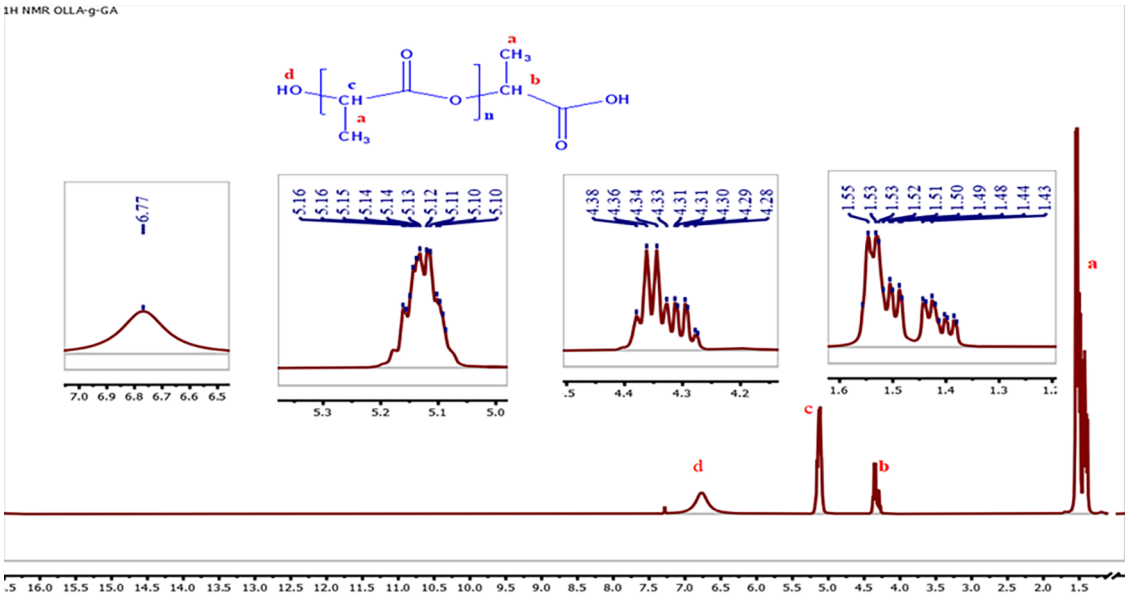

Figure 2: ^{1}H-NMR spectra of OLLA.

The ^{1}H-NMR Spectrum of OLLA-g-GA (Fig. 3), exhibits that the signal corresponding to O-H signal at δ 1.38–1.58 ppm shows a reduction in the number of doublet peaks and is shifted upfield compared to the OLLA resonance peak. This change confirms the partial consumption of hydroxyl groups due to ester formation. The backbone methine multiplet of OLLA at δ 5.07–5.16 ppm diminished in intensity, supporting the conclusion that CH groups in the lactic acid oligomer chain decrease upon conjugation. Peaks around δ 4.28–4.34 ppm exhibit some split formation and broadening, which suggests that there are altered chemical environment and an asymmetric structure within the overall backbone of the compound [20]. These spectral changes confirm that OLLA chains are covalently bonded to GA, resulting in the formation of the desired grafted compound.

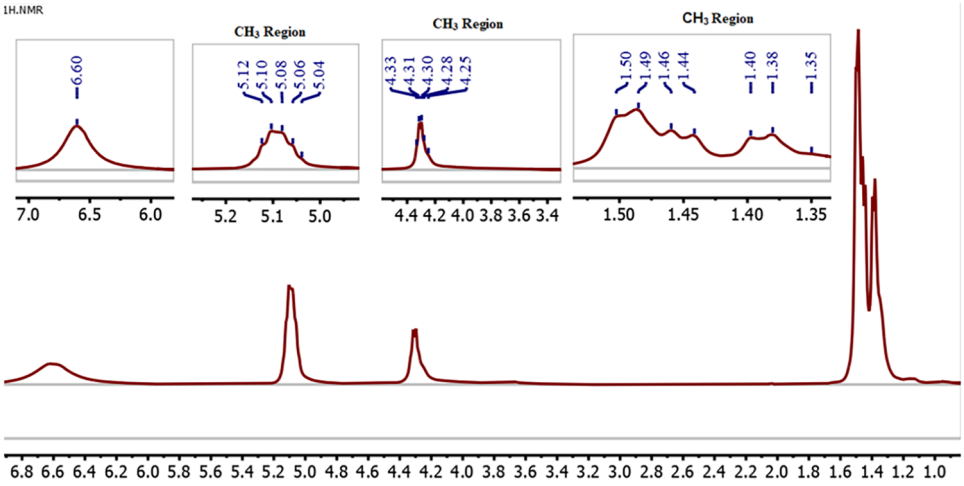

Figure 3: ^{1}H NMR spectra of OLLA-g-GA.

The ^{1}H NMR spectrum for *Euphorbia trigona* Mill latex (ETML) displays characteristic polyisoprene features as illustrated in Fig. 4. A broad multiplet appears near δ 0.73–1.23 ppm attributed to the methylene and methyl protons along the polymer chain. Distinct doublets at δ 1.47–1.65 ppm, including at δ 1.48, 1.51, 1.53 and 1.55 ppm corresponding to methyl groups adjacent to unsaturated carbons. A singlet at δ 2.07 ppm is assigned to methyl groups adjacent to unsaturated carbons. Overall, these chemical shifts confirm that ETML consists of polyisoprene and are consistent with the structure of natural rubber [21].

The ^^{1}H NMR spectrum of modified ETML (Fig. 5) reveals distinct changes compared to native ETML, confirming successful grafting with lactic acid oligomers. Increased intensity and the appearance of additional doublet and singlet peaks in the CH_3 region (1.35–1.65 ppm) indicate the incorporation of methyl groups from the grafted oligomer. A significant reduction in the intensity of methine signals at 5.08–5.21 ppm, originally attributed to polyisoprene CH groups, suggests carboxylation and structural modification of the internal backbone. New peaks at 4.36 and 4.37 ppm correspond to methine protons of the lactic acid oligomer. Furthermore, the emergence of signals within the 2.28–3.28 ppm range is consistent with ester bond formation.

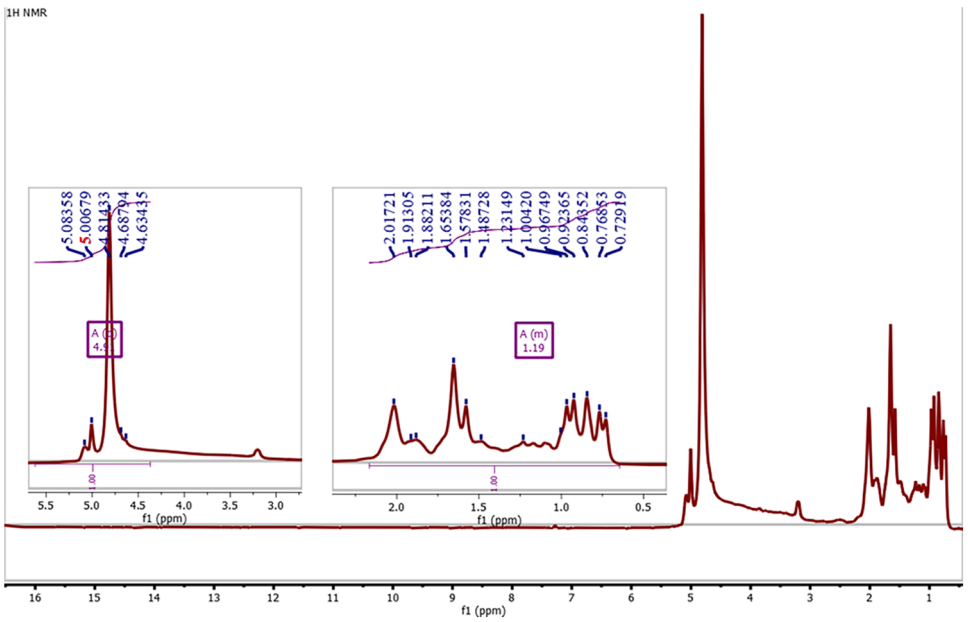

Figure 4: ^{1}H NMR of ETML.

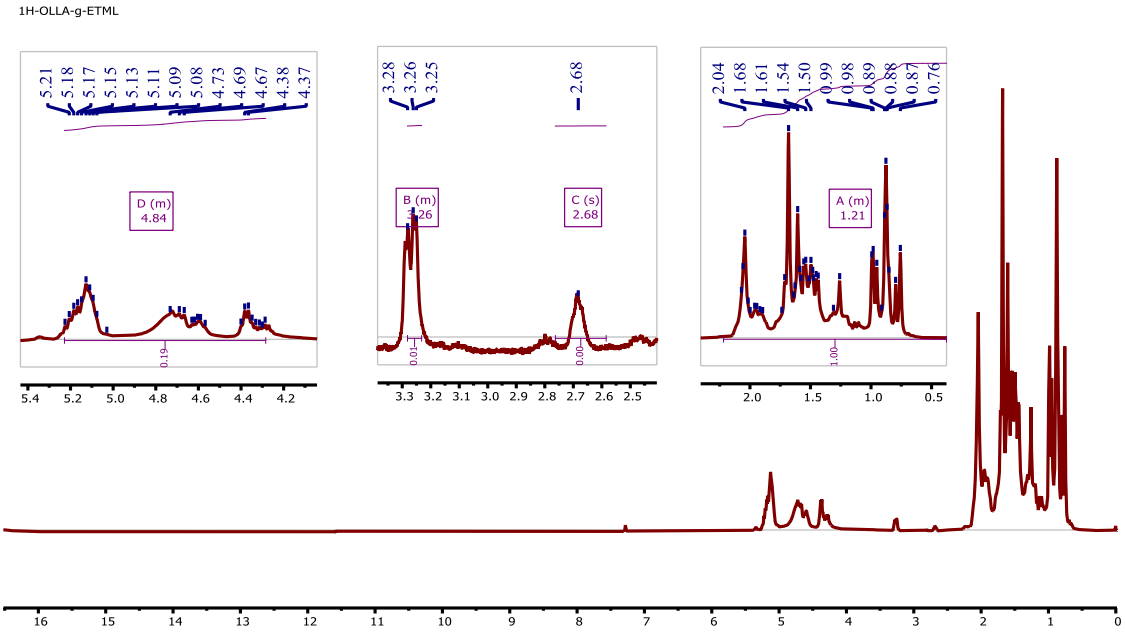

Figure 5: ^{1}H NMR spectra of OLLA-g-ETM bio-conjugate.

3.3 FTIR Analysis of Chemical Interactions in PLA Bio-Composites

Fig. 6 illustrates the FTIR spectra of PLA and PLA-based composite (PLA/OLLA-g-GA, PLA/OLLA-g-ETML and PLA/masterbatch) recorded before and after thermal annealing. Neat PLA shows characteristics bands corresponding to O-H stretching at region of 3500–3200 cm^{-1}, strong ester carbonyl stretching in the region of 1750–1760 cm^{-1}, in the region of bending vibrations of CH_3 (1450–1380 cm^{-1}) and C-O-C stretching

bands in the region of 1180–1080 cm^{-1}. There is no new peak exhibited in thermally annealed PLA, however slight peaks sharpening is observed, which suggests increased molecular ordering and crystallinity [22].

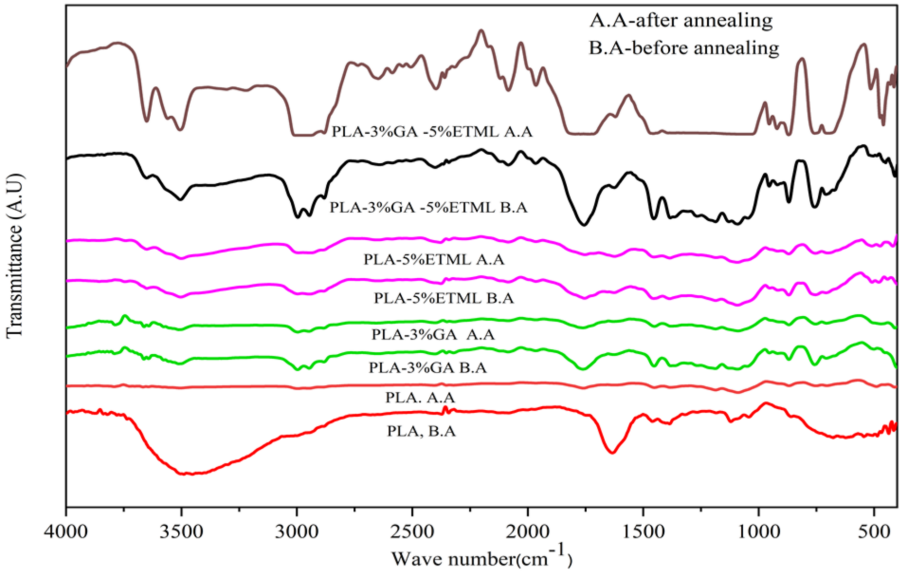

Figure 6: FTIR of neat PLA and PLA/master batch bio-composite before and after annealing.

The PLA/OLLA-g-GA, PLA/OLLA-g-ETML composite retains the main PLA bands, proving the absence of chemical interaction or modification, while the increased intensity and broadening of the hydroxyl band indicate the presence of a large amount of O-H group on additives [23]. A small change in the carbonyl band suggests a hydrogen bond interaction of PLA with bio-fillers. The same effect is more pronounced in the PLA/masterbatch system, where interfacial compatibility was improved due to the combined effect of modified ETML and GA. Spectral comparison shows the absence of new groups and so it can be said that the structure is thermally stable and annealing improves band definition. In summary, the analysis of FTIR spectroscopy will indicate that GA and ETML interact with PLA physically through hydrogen bonding, while annealing enhances molecular ordering without inducing chemical degradation.

3.4 Mechanical Properties of PLA Bio-Composites

Fig. 7 presents the tensile strength and elongation at break of neat PLA and its biocomposites with modified GA, ETML, and their combined (masterbatch). Neat PLA exhibits the lowest tensile strength and elongation at break due to its inherent brittleness. The addition of 3 wt% OLLA-g-GA substantially improves the tensile strength of PLA. This can be ascribed to the stress transfer between PLA and GA and the improved interfacial adhesion [24]. On the other hand, PLA that is reinforced with 5 wt% OLLA-g-ETML shows a much greater improvement in elongation at break with a moderate increase in tensile strength. This reflects the more plasticizing and toughening effect of modified ETML which enhances chain movement.

A synergistic reinforcing effect is observed. This is likely due to improved dispersion and stronger physical interactions within the matrix, which is contributed to the highest tensile strength of the PLA/masterbatch (modified 3% GA–5% ETML) [25]. While the masterbatch composite elongation at break is slightly lower than that of the PLA–ETML, it is still greater than that of neat PLA. This indicates an improvement in strength and flexibility [26]. With respect to the results, it can be concluded that GA is the major source of the increase in stiffness and strength, while the ETML is the cause of the increased ductility, and that both were added synergistically to optimize the mechanical properties.

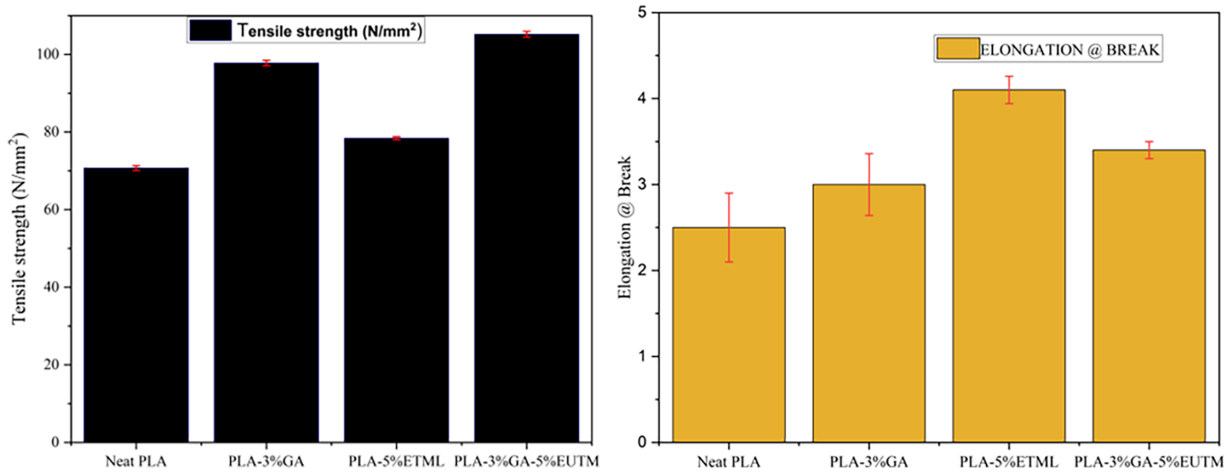

Figure 7: Tensile strength and elongation at break of Neat PLA and its biocomposite.

3.5 Differential Scanning Calorimetry

Differential scanning calorimetry (DSC) was used to study the thermal transitions and crystallisation nature of neat PLA and PLA-based composites under non-isothermal conditions. A series of measurements were taken using a heating–cooling–heating sequence. Initially, during the first heating stage, the samples were heated to a temperature above the melting temperature of PLA in order to eliminate the prior thermal history. The samples were cooled to room temperature and reheated to check for the glass transition temperature (Tg), melting temperature (Tm), melting enthalpy (ΔHm), and degree of crystallinity (Xc).

The degree of crystallinity was calculated from the melting enthalpy alone, using Eq. (3) for neat PLA and Eq. (4) for PLA composites, and not subtracting any cold crystallization [20,27,28]. This strategy works under the premise that most samples were highly crystallized (implying either slowly cooled or annealed), and thus would have a very low contribution of cold crystallisation. A good comparative estimate of the relative crystallinity for the composites was achieved using this methodology.

The crystallisation behavior of PLA was significantly influenced by the addition of OLLA-g-GA, OLLA-g-ETML, and their masterbatch. The oligomeric lactic acid component grafted enhanced chain mobility and, thus, acted as a plasticizer, while the bio-based modifiers functioned as heterogeneous nucleation sites [29]. Modified GA and ETML components in the masterbatch showed nucleating contribution, as the mixture promoted crystallisation to a greater extent than either additive acting alone. This is due to increased nucleation sites, better dispersion, and increased mobility of molecular segments [30]. This combined nucleation–plasticization mechanism caused a greater reduction in Tg and crystallinity in the OLLA-g-GA, OLLA-g-ETML and masterbatch modified PLA. However, the PLA modified with masterbatch showed the greatest crystallisation due to the combined nucleation–plasticization effect of the additives.

The proposed nucleation mechanism of OLLA-g-GE, OLLA-g-ETML composites, and their masterbatch is presented in Fig. 8. The self-assembled nucleating domains act as heterogeneous nucleation sites, enhancing crystal formation and growth by lowering barrier energy [28]. However, in the absence of DSC cooling DSC experiment, isothermal crystallisation kinetics, or structural analysis techniques, definitive crystallization cannot be confirmed. The degree of crystallinity (X_c) was calculated from the melting enthalpy (ΔHm) without subtracting the cold crystallisation enthalpy (ΔHcc) to facilitate comparison of relative crystallisation behavior under identical thermal histories. Similar approaches have been reported for annealing and nucleation induced crystallization of PLA [31,32].

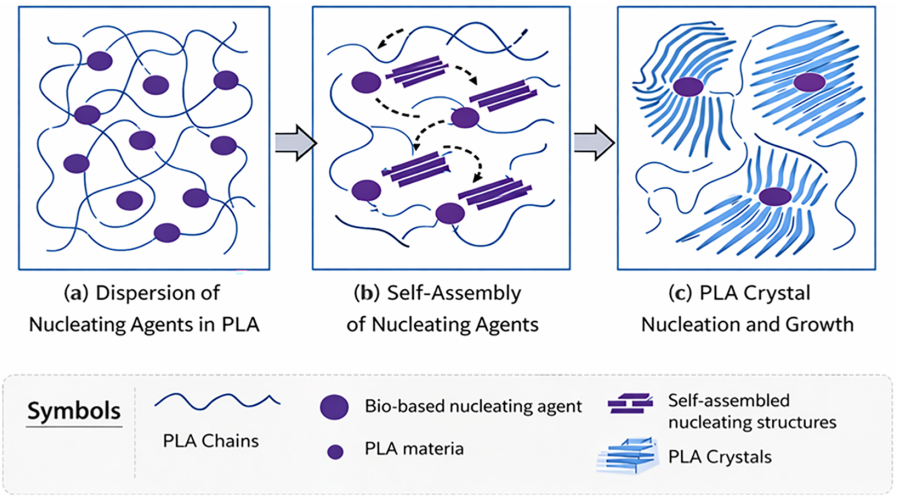

Figure 8: Illustration of the crystallization process of PLA initiated by bio-filler nucleating agent.

The PLA/OLLA-g-GA and PLA/OLLA-g-ETML also had a lower Tg than neat PLA, corroborating the presence of the oligomeric component, which increased chain mobility, in contrast, the PLA/masterbatch composites had a slight change in Tg and Tm, showing that the masterbatch formulation struck a favorable compromise between nucleation efficiency and thermal stability. DSC thermograms of the neat PLA and PLA-based bio-composites are shown in Fig. 9. Thermal parameters including glass transition temperature (Tg), melting temperature (Tm), melting enthalpy (ΔHm), and degree of crystallinity (Xc) were tabulated in Table 3. Crystal growth and perfection were promoted by annealing selected samples at 110°C for 150 min. For neat PLA, the degree of crystallinity increased from 31.36% to 39.32%, 36.30% and 40.39% of Neat PLA, PLA/OLLA-g-GA, PLA/OLLA-g-ETML and PLA/masterbatch composites, respectively, which clearly showed the dominant nucleation efficiency and the synergistic effect of the masterbatch system.

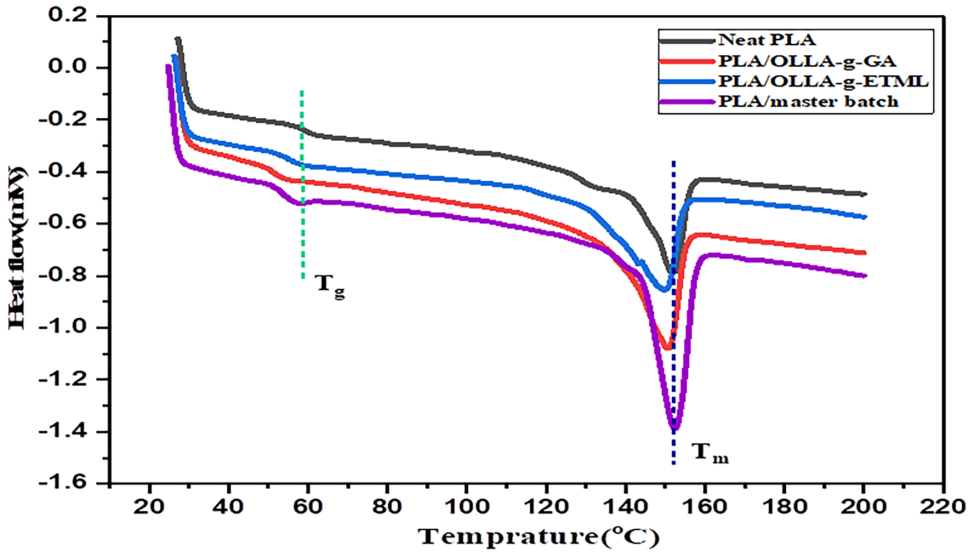

Figure 9: DSC thermo grams of neat PLA and PLA/bio composites.

Table 3: Calculated degree of crystallinity of neat PLA and PLA based bio-composite.

Sample	T_g (°C)	ΔH_m (J/g)	T_m (°C)	X_c (%)
Neat PLA	57.43	29.16	151.59	31.36
PLA/OLLA-g-GA	49.72	36.575	150.55	39.32
PLA/OLLA-g-ETML	52.16	33.72	149.64	36.30
PLA/master batch	51.35	43.1	152.25	40.39

3.6 Effect of Thermal Annealing and Annealing Time on Crystallization Behavior of PLA and PLA-Biocomposite

Thermal annealing of PLA conducted above the glass transition temperature and below the melting temperature significantly affected the crystalline structure and thermal behavior. As illustrated in Fig. 10 and Table 4 thermal annealing of PLA at 110°C for 2.5 h resulted in significant changes in thermal transitions. The glass transition temperature (Tg) decreased from 61.6°C to 56.71°C, which may be attributed to increased molecular mobility in the amorphous region by recrystallisation and relaxation behaviour. This typical behavior is commonly observed in a system with annealed PLA systems and is related to improved ductility.

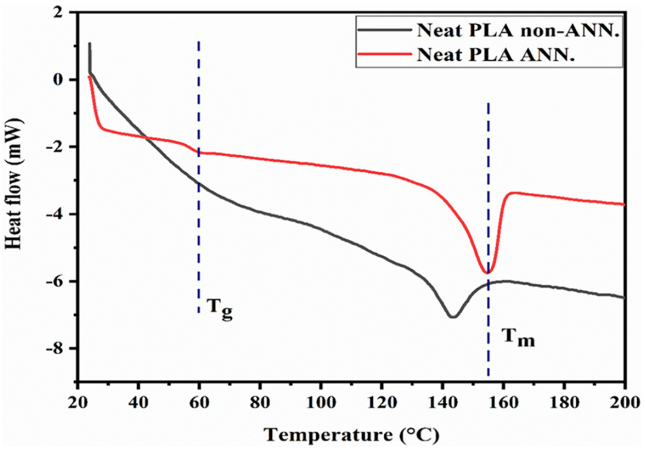

Figure 10: DSC thermograms of neat PLA with and without annealing.

Table 4: Calculated degree of crystallinity of neat PLA with and without annealing.

Sample	T_g (°C)	ΔH_m (J/g)	T_m (°C)	X_c (%)
Neat PLA (non-annealed)	65.6°C	23.4	143	31.36
Neat PLA (annealed)	57.43	29.16	151.59	35.28

Annealing also raises the melting temperature Tm of the PLA from 143°C to 151.59°C, due to the more stable and perfect crystalline arrangements which lead to more ordered [33]. Moreover, annealing boosts the degree of crystallinity of PLA, resulting from improved chain alignment and crystal growth enhanced by sufficient molecular mobility at the thermal annealing temperature [34]. There is also good agreement with previous reports on the impact of thermal annealing on the degree of crystallisation and thermal characteristics [35]. Overall, thermal annealing improves the degree of crystallinity and the perfection of crystal structures, thermal annealing manages to refine the structural and characteristics of the PLA to meet the required application [36].

Similarly, the DSC thermograms of PLA-based biocomposite systems are shown in Fig. 11, and corresponding thermal parameters are summarized in Table 5. The values of thermal parameters Tg, ΔHm, Tm and the degree of crystallinity (Xc) were influenced by the duration of annealing. For the PLA/OLLA-g-GA biocomposite, Xc increased from 38.77% to 44.20% with the increasing annealing times, indicating enhanced crystallisation due to improved chain rearrangement and nucleation during heat treatment. The enhancement in the degree of crystallinity is expected to improve tensile strength and stiffness by introducing more crystalline domains.

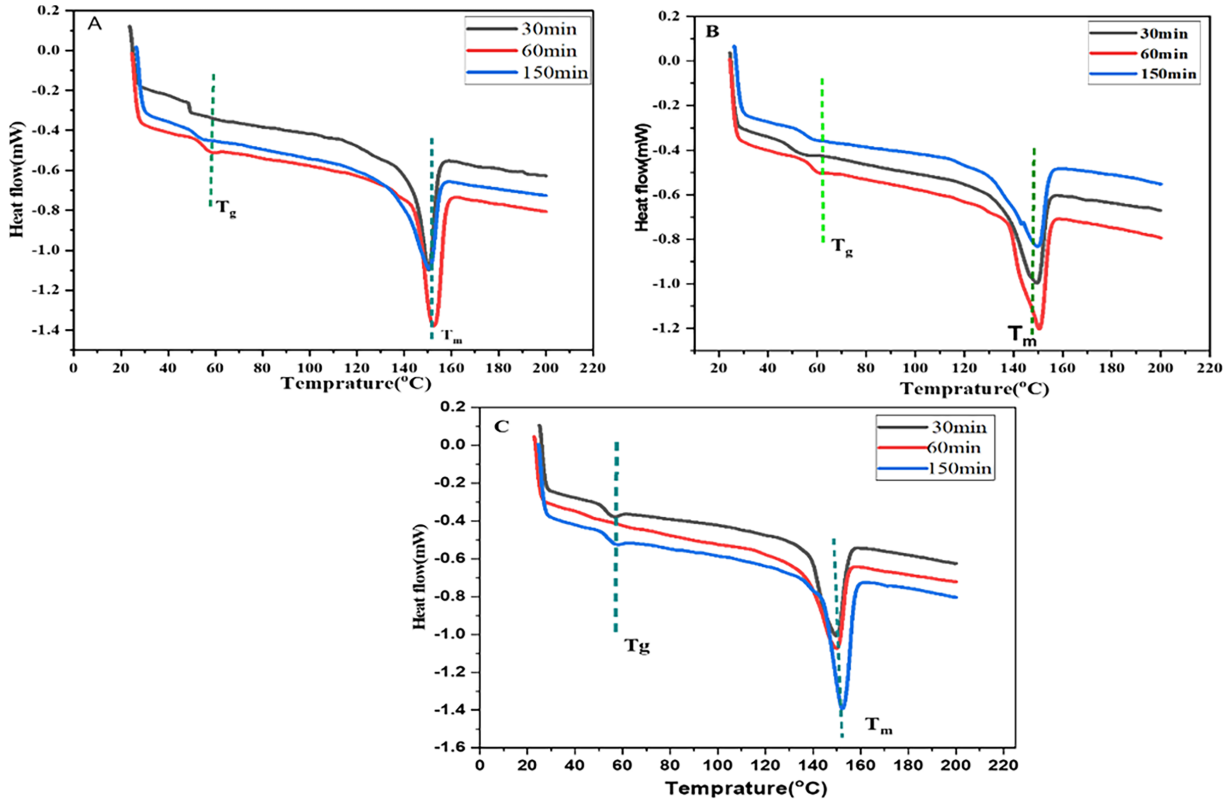

Figure 11: DSC thermograms of (**A**) PLA/OLLA-g-GA, (**B**) PLA/OLLA-g-ETML and (**C**) PLA/master batch bio composites.

Table 5: Effects of annealing time on the degree of crystallinity of PLA.

Sample Code	Time (min)	T_g (°C)	ΔH_m (J/g)	T_m (°C)	X_c (%)
PLA/OLLA-g-GA	30	48.42	34.2	150.34	38.77
	60	49.2	38.34	152.41	41.22
	90	48.9	39.45	150.55	44.2
PLA/OLLA-g-ETML	30	46.66	33.71	149.3	37.6
	60	53.784	36.13	150.32	39.84
	90	51.32	34.34	149.64	37.96

(Continued)

Table 5 (continued)

Sample Code	Time (min)	T_g (°C)	ΔH_m (J/g)	T_m (°C)	X_c (%)
PLA/master batch	30	51.095	40.28	152.23	40.3
	60	51.54	33.6	149.74	43.12
	90	51.95	41.7	152.25	45.83

In comparison, PLA/OLLA-G-ETML exhibited an increase in Xc at intermediate annealing time (37.60% to 39.84%) attained Xc followed by a slight reduction at longer periods of annealing. This behavior suggests a dominant plasticizing effect of OLLA-g-ETML, resulting in a decline in the stable crystal growth elements at increased molecular mobility. The concurrent reduction in Tg further suggests that enhancement chain flexibility, which is typically associated with improved ductility with lower crystallinity crystalline at higher annealing time. For the PLA/masterbatch system, Xc increased from 40.30% to 45.83% with increased time of annealing, which possibly suggests the presence of uniform dispersion of the masterbatch within the PLA matrix. This positive variation is likely to be linked with the improvement of nucleation on the master batch system. This enhances thermal performance, particularly tensile strength and thermal resistance.

3.7 Thermo Gravimetric Analysis (TGA)

Thermal analysis using TGA was conducted to assess the thermal decomposition behavior of neat PLA and biocomposites are shown in Fig. 12. All the samples exhibit a single-step degradation behavior occurring between 300°C and 420°C, characteristic of PLA backbone scission. Neat PLA shows the onset of major thermal degradation at around 330°C, followed by rapid mass loss with nearly complete decomposition above 400°C [37]. A small initial mass loss below 150°C is observed for neat PLA, which can be attributed to the evaporation of physically adsorbed moisture and low-molecular-weight volatile residues [38]. This early weight loss is negligible for the biocomposite samples, indicating improved moisture resistance after modification.

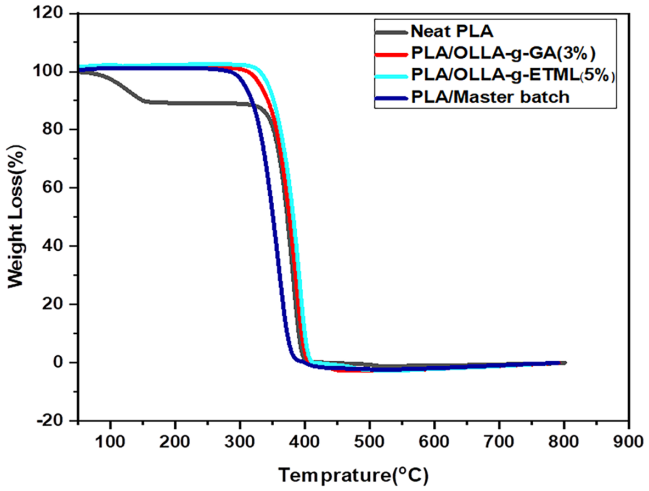

Figure 12: Thermal degradation curve of NPLA and PLA/master batch bio composite.

In the thermal degradation of neat PLA, the degradation began at 330°C, followed by rapid mass loss with nearly complete decomposition above 400°C. A minor mass loss at nearly 150°C is exhibited for neat

PLA, which is attributed to the release of adsorbed moisture and evaporation of low-molecular-weight volatile decomposition residues. On the other hand, the biocomposites showed little early weight loss, which indicates an improvement in moisture resistance following modification.

PLA/OLLA-g-ETML (5%) had the highest overall thermal stability among the biocomposites, as evidenced by a delayed onset of degradation and a shift to a higher temperature when compared to neat PLA, PLA/masterbatch, and PLA/OLLA-g-ETML [39]. As previously stated, the higher thermal stability is attributed to stronger interfacial interactions between PLA and modified ETML [40,41]. This constraint in chain mobility induced a temperature delay in molecular chain scission, keeping chains of PLA components together. Furthermore, the enhanced degree of crystallinity shown by DSC analysis contributes to thermal stability at high temperatures.

However, the PLA/masterbatch was thermally unstable, with an earlier onset of degradation and a steeper mass-loss curve. The master batch's considerably higher crystallinity is attributable in part to the thermal stability of the reactive grafted species and the residual low-molecular-weight species. The low-molecular-weight ingredients can catalyze PLA chain scission and initiate breakdown at lower temperatures. This indicates that the balance of crystallinity swings toward a lack of chemical stability in this system.

Overall, the TGA results show that both the crystallinity and the stability of the chemical composition of the modifiers influence the thermal stability of PLA-based systems. PLA/OLLA-g-ETML has the highest thermal stability, demonstrating the advantages of ETML grafting. The decreased stability of the masterbatch illustrates how the chemically active species might encourage PLA's heat degradation, demonstrating their detrimental impacts. The detailed thermogravimetric parameters of PLA and the PLA-based bio-composites are presented in Table 6.

Table 6: TGA analysis of PLA and PLA-based bio-composite.

Sample Code	T10% Weight Loss (°C)	T50% Weight Loss (°C)	Tmax Rate of Degradation (°C)	T (°C)
PLA	321	367	386.09	380.5
PLA/OLLA-*g*-GA (3%)	348	381.5	386.7	392.67
PLA/OLLA-*g*-ETML (5%)	353	384.9	392.51	398
PLA/Master batch	318	354	359	374

4 Conclusions

The successful addition of oligomeric lactic acid (OLLA) to Gum Arabic (GA) and *Euphorbia trigona* Mill latex (ETML) was confirmed qualitatively with NMR spectroscopy. The grafting process was further quantified using the percentage of grafting (GP) and percentage of grafting efficiency (GE) with OLLA-g-GA demonstrating 21.5 ± 0.56% GP and 67.2 ± 0.89% GE while OLLA-g-ETMLA showed 24.3 ± 0.33% GP and 73.6 ± 0.47% GE. FTIR analysis confirmed that the chemical backbone of the PLA was maintained, while the hydroxyl-rich bio-additives interacted with PLA through polar hydrogen bonding, thereby enhancing interfacial compatibility. The increased molecular ordering induced by annealing was also shown with the sharpening of the carbonyl and C–O–C peaks.

Mechanical testing also showed that 3 wt% OLLA-g-GA increased the tensile strength due to improved stress transfer but with 5 wt% OLLA-g-ETML, it showed an elongation at break improvement because of the plasticizing effects. The combined masterbatch (3 wt% GA + 5 wt% ETML) exhibited the greatest tensile strength due to synergistic reinforcement, while also showing improvement of ductility. The grafted

bioconjugates also acted as nucleating agents, increasing the crystallinity of PLA from 29.16% for neat PLA to 44%, 37.96%, and 45.83% for PLA/OLLA-g-GA, PLA/OLLA-g-ETML, and the masterbatch system, respectively. A small Tg change was observed, and the TGA demonstrated single-step degradation while also having very slight reductions in thermal stability of the masterbatch system.

The grafted bioconjugates acted as effective nucleating agents, increasing the crystallinity of PLA to 38.77%, 37.96%, 45.83%, with OLLA-g-GA, OLLA-g-ETML and the masterbatch, respectively, while thermal annealing increases the degree of crystallinity. The shift in *Tg* and *Tm* was very slight, and TGA revealed that the masterbatch system degraded in single-step degradation with only a slight decrease in thermal stability. In general, NMR, FTIR, grafting, mechanical, and thermal analyses show that OLLA-g-GA and OLLA-g-ETML bio-conjugates act synergistically to improve the crystallinity, mechanical performance, and functional properties of PLA without compromising thermal stability, pointing to their future use as sustainable and functional materials.

Acknowledgement: The authors acknowledge the support of Adama Science and Technology University for providing access to university facilities, library resources, internet services, and a conducive research environment during the preparation of this manuscript.

Funding Statement: The authors received no specific funding for this study.

Author Contributions: Kasahun Tsegaye Mekonnen: investigation, methodology, conceptualization, formal analysis, writing—original draft; Melaku Tesfaye Alemea: supervision, methodology, validation, visualization, resource; Dessie Ezez: conceptualization, formal analysis, validation, writing—review and editing; Abenezer Zenebe: writing review; Negussie Darota Daka: editing. All authors reviewed and approved the final version of the manuscript.

Availability of Data and Materials: Data available on request from the authors. The data that support the findings of this study are available from the Corresponding Author, [Kasahun Tsegaye Mekonnen] upon reasonable request.

Ethics Approval: Not applicable. This study did not involve human participants or animals.

Conflicts of Interest: The authors declare no conflicts of interest.

References

1. Samuel HS, Ekpan FM, Ori MO. Biodegradable, recyclable, and renewable polymers as alternatives to traditional petroleum-based plastics. Asian J Environ Res. 2024;1(3):152–65. doi:10.69930/ajer.v1i3.86.
2. Rajendran S, Al-Samydai A, Palani G, Trilaksana H, Sathish T, Giri J, et al. Replacement of petroleum based products with plant-based materials, green and sustainable energy—a review. Eng Rep. 2025;7(4):e70108. doi:10.1002/eng2.70108.
3. Ntrivala MA, Pitsavas AC, Lazaridou K, Baziakou Z, Karavasili D, Papadimitriou M, et al. Polycaprolactone (PCL): the biodegradable polyester shaping the future of materials—a review on synthesis, properties, biodegradation, applications and future perspectives. Eur Polym J. 2025;234(28):114033. doi:10.1016/j.eurpolymj.2025.114033.
4. Wu Y, Gao X, Wu J, Zhou T, Nguyen TT, Wang Y. Biodegradable polylactic acid and its composites: characteristics, processing, and sustainable applications in sports. Polymers. 2023;15(14):3096. doi:10.3390/polym15143096.
5. Naser AZ, Deiab I, Darras BM. Poly(lactic acid) (PLA) and polyhydroxyalkanoates (PHAs), green alternatives to petroleum-based plastics: a review. RSC Adv. 2021;11(28):17151–96. doi:10.1039/d1ra02390j.
6. Ilyas RA, Sapuan SM, Harussani MM, Hakimi MYAY, Haziq MZM, Atikah MSN, et al. Polylactic acid (PLA) biocomposite: processing, additive manufacturing and advanced applications. Polymers. 2021;13(8):1326. doi:10.3390/polym13081326.
7. Valapa R, Hussain S, Iyer PK, Pugazhenthi G, Katiyar V. Influence of graphene on thermal degradation and crystallization kinetics behaviour of poly(lactic acid). J Polym Res. 2015;22(9):175. doi:10.1007/s10965-015-0823-2.

8. Aminyan R, Garmabi H, Katbab AA. Supertough shape memory bionanocomposites of thermoplastic vulcanizates based on PLA-EVA and cellulose nanocrystal. J Polym Environ. 2024;32(10):5272–89. doi:10.1007/s10924-024-03309-2.
9. Mat Piah MB, Ahmad MN, Abdullah EN, Muzakkar MZ. Modifications of poly(lactic acid) with blends and plasticization for tenacity and toughness improvement. Indones J Chem. 2023;23(4):1161. doi:10.22146/ijc.80830.
10. Uddin MH, Mulla MH, Abedin T, Manap A, Yap BK, Rajamony RK, et al. Advances in natural fiber polymer and PLA composites through artificial intelligence and machine learning integration. J Polym Res. 2025;32(3):76. doi:10.1007/s10965-025-04282-7.
11. Sharma C, Kundu S, Singh S, Saxena J, Gautam S, Kumar A, et al. From concept to shelf: engineering biopolymer-based food packaging for sustainability. RSC Sustain. 2025;3(11):4992–5026. doi:10.1039/d5su00483g.
12. Bavaliya KJ, Vala NS, Raj M, Raj L. A review on biodegradable composites based on poly(lactic acid) with various bio fibers. Chem Pap. 2024;78(5):2695–728. doi:10.1007/s11696-023-03298-x.
13. Tazwar HT, Antora MF, Rahman MZ. Functionalization strategies for sustainable plant fiber composites: a comprehensive review of techniques, performance and future directions. J Mater Res Technol. 2025;38(5):1083–102. doi:10.1016/j.jmrt.2025.07.237.
14. Coudane J, Nottelet B, Mouton J, Garric X, Van Den Berghe H. Poly(ε-caprolactone)-based graft copolymers: synthesis methods and applications in the biomedical field: a review. Molecules. 2022;27(21):7339. doi:10.3390/molecules27217339.
15. Tripathi N, Katiyar V. PLA/functionalized-gum Arabic based bionanocomposite films for high gas barrier applications. J Appl Polym Sci. 2016;133(21):43458. doi:10.1002/app.43458.
16. Borkotoky SS, Ghosh T, Bhagabati P, Katiyar V. Poly (lactic acid)/modified gum Arabic (MG)based microcellular composite foam: effect of MG on foam properties, thermal and crystallization behavior. Int J Biol Macromol. 2019;125:159–70. doi:10.1016/j.ijbiomac.2018.11.257.
17. Wasie Y, Periyasamy S, Tesfaye M. Lactic acid oligomer grafted gum acacia encapsulated controlled release nitrogen fertilizer for crops improvements and greener soil sustainability. South Afr J Chem Eng. 2025;53(10):158–75. doi:10.1016/j.sajce.2025.04.017.
18. Song L, Zhang Q, Hao Y, Li Y, Chi W, Cong F, et al. Effect of different comonomers added to graft copolymers on the properties of PLA/PPC/PLA-g-GMA blends. Polymers. 2022;14(19):4088. doi:10.3390/polym14194088.
19. Tripathi N, Katiyar V. Lactic acid oligomer (OLLA) grafted gum Arabic based green adhesive for structural applications. Int J Biol Macromol. 2018;120(Pt A):711–20. doi:10.1016/j.ijbiomac.2018.07.199.
20. Nagarajan V, Zhang K, Misra M, Mohanty AK. Overcoming the fundamental challenges in improving the impact strength and crystallinity of PLA biocomposites: influence of nucleating agent and mold temperature. ACS Appl Mater Interfaces. 2015;7(21):11203–14. doi:10.1021/acsami.5b01145.
21. Zahir L, Kida T, Tanaka R, Nakayama Y, Shiono T, Kawasaki N, et al. Synthesis of thermoplastic elastomers with high biodegradability in seawater. Polym Degrad Stab. 2021;184:109467. doi:10.1016/j.polymdegradstab.2020.109467.
22. Rifa'i AF, Kaavessina M, Distantina S. Evaluation of the chemical structure and thermal properties of polyethylene glycol (PEG)-doped polylactic acid (PLA)/multiwalled carbon nanotube (MWCNT) composites. Indones J Chem Anal. 2024;7(2):66–76. doi:10.20885/ijca.vol7.iss2.art5.
23. Vengadesan E, Morakul S, Muralidharan S, Pullela PK, Alarifi A, Arunkumar T. Enhancement of polylactic acid (PLA) with hybrid biomass-derived rice husk and biocarbon fillers: a comprehensive experimental study. Discov Appl Sci. 2025;7(3):161. doi:10.1007/s42452-025-06583-4.
24. N'Gatta KM, Belaid H, El Hayek J, Assanvo EF, Kajdan M, Masquelez N, et al. 3D printing of cellulose nanocrystals based composites to build robust biomimetic scaffolds for bone tissue engineering. Sci Rep. 2022;12(1):21244. doi:10.1038/s41598-022-25652-x.
25. Nagy B, Miskolczi N, Eller Z. Improving mechanical properties of PLA/starch blends using masterbatch containing vegetable oil based active ingredients. Polymers. 2021;13(17):2981. doi:10.3390/polym13172981.

26. Agbakoba VC, Hlangothi P, Andrew J, John MJ. Preparation of cellulose nanocrystal (CNCs) reinforced polylactic acid (PLA) bionanocomposites filaments using biobased additives for 3D printing applications. Nanoscale Adv. 2023;5(17):4447–63. doi:10.1039/d3na00281k.
27. Homklin R, Hongsriphan N. Mechanical and thermal properties of PLA/PBS co-continuous blends adding nucleating agent. Energy Proc. 2013;34(4):871–9. doi:10.1016/j.egypro.2013.06.824.
28. Jiang L, Shen T, Xu P, Zhao X, Li X, Dong W, et al. Crystallization modification of poly(lactide) by using nucleating agents and stereocomplexation. E Polym. 2016;16(1):1–13. doi:10.1515/epoly-2015-0179.
29. Obasa VD, Olanrewaju OA, Owoyemi IO, Adeosun SO. Evaluation of the mechanical, thermal, and microstructural behaviour of gum Arabic reinforced polylactide (PLA) composite. J Mater Sci Compos. 2025;6(1):14. doi:10.1186/s42252-025-00079-5.
30. Oliver-Ortega H, Tresserras J, Julian F, Alcalà M, Bala A, Espinach FX, et al. Nanocomposite materials of PLA reinforced with nanoclays using a masterbatch technology: a study of the mechanical performance and its sustainability. Polymers. 2021;13(13):2133. doi:10.3390/polym13132133.
31. Day M, Nawaby AV, Liao X. ADSC study of the crystallization behaviour of polylactic acid and its nanocomposites. J Therm Anal Calorim. 2006;86(3):623–9. doi:10.1007/s10973-006-7717-9.
32. Liu W, Wu X, Chen X, Liu S, Zhang C. Flexibly controlling the polycrystallinity and improving the foaming behavior of polylactic acid via three strategies. ACS Omega. 2022;7(7):6248–60. doi:10.1021/acsomega.1c06777.
33. Elnabawy E, Sun D, Shearer N, Toptaş A, Kılıç A, Shyha I. The role of annealing in enhancing crystallinity, mechanical properties, piezoelectricity, and air filtration performance of polylactic acid nanofibers. Mater Chem Phys. 2025;343:131000. doi:10.1016/j.matchemphys.2025.131000.
34. da Silva FU, Luna CBB, da Silva FS, Barreto JVM, Schmitz DP, Soares BG, et al. Exploring the effect of annealing on PLA/carbon nanotube nanocomposites: in search of efficient PLA/MWCNT nanocomposites for electromagnetic shielding. Polymers. 2025;17(2):246. doi:10.3390/polym17020246.
35. Diani J, Liu Y, Gall K. Finite strain 3D thermoviscoelastic constitutive model for shape memory polymers. Polym Eng Sci. 2006;46(4):486–92. doi:10.1002/pen.20437.
36. Pérez-Fonseca AA, Robledo-Ortíz JR, González-Núñez R, Rodrigue D. Effect of thermal annealing on the mechanical and thermal properties of polylactic acid–cellulosic fiber biocomposites. J Appl Polym Sci. 2016;133(31):43750. doi:10.1002/app.43750.
37. Ainali NM, Tarani E, Zamboulis A, Črešnar KP, Zemljič LF, Chrissafis K, et al. Thermal stability and decomposition mechanism of PLA nanocomposites with kraft lignin and tannin. Polymers. 2021;13(16):2818. doi:10.3390/polym13162818.
38. Ruz-Cruz MA, Herrera-Franco PJ, Flores-Johnson EA, Moreno-Chulim MV, Galera-Manzano LM, Valadez-González A. Thermal and mechanical properties of PLA-based multiscale cellulosic biocomposites. J Mater Res Technol. 2022;18:485–95. doi:10.1016/j.jmrt.2022.02.072.
39. Bernardes GP, Andrade MP, Poletto M, Luiz NR, Santana RMC, Forte MMDC, et al. Evaluation of thermal decomposition kinetics of poly (lactic acid)/ethylene elastomer (EE) blends. Polymers. 2023;15(21):4324. doi:10.3390/polym15214324.
40. Musa AA, Bello A, Adams SM, Onwualu AP, Anye VC, Bello KA, et al. Nano-enhanced polymer composite materials: a review of current advancements and challenges. Polymers. 2025;17(7):893. doi:10.3390/polym17070893.
41. Khan ZI, Ali Mohsin ME, Habib U, Mousa S, Safdar Hossain SK, Ali SS, et al. Enhanced mechanical and thermal performance of sustainable RPET/PA-11/joncryl® nanocomposites reinforced with halloysite nanotubes. Polymers. 2025;17(11):1433. doi:10.3390/polym17111433.